

Thermal Effects Analysis of GTAW and FCAW Welds on the SS400 Steel

Kyung-Hyen Lee¹, Sueng-Dai Kim^{*2}, Bo-An Kang³

¹Professor, Department of Industrial Facility, Korea Polytechnics University, PoHang, Korea.

^{*2}Professor, Department of Mechanical System Engineering, Nambu University, Gwang-Ju, Korea.

³Professor, Department of Electrical Engineering, Nambu University, GwangJu, Korea.

asas7513@naver.com¹, sdkim@nambu.ac.kr^{*2}, bakang@nambu.ac.kr³

Article Info

Volume 83

Page Number: 4349 - 4360

Publication Issue:

March - April 2020

Abstract

The thermal effects on the gas tungsten arc and flux cored arc welded specimens using SS400 mild steel was analyzed. Heat transfer and residual stress results were used to compare the advantages and disadvantages of each welding method in terms of efficiency. When joining SS400 mild steel plate by V-butt welding, the heat affected zones and heat distribution characteristics of the two specimens welded with GTAW and FCAW were compared according to the welding method and number of passing layers. In the GTAW, main welding was followed after temporary welding using a TIG welder. FCAW used a CO₂ welder under rating current 350A. In order to observe the change due to heat, heat transfer and residual stress analysis of each specimen were performed. In the GTAW specimens, the width of the heat affected zone was narrow and there was no change in the weld bead structure. Coarse dendrite tissue was observed in FCAW specimens. This is thought to be due to the difference in cooling rate that occurs between the weld base material and the molten structure. The difference in residual stress of the specimens applied by the two welding methods was not significant. The residual stress was higher in the FCAW method than in the GTAW method. In the case of the FCAW method, the residual stresses were high even in one pass welding, and this result seems to be due to the high current welding. In general, high tensile stress is concentrated around the weld bead, but as the distance from the bead increases, the tensile stress decreases. In the future, the thermal elasto-plastic analysis is conducted by dividing the model applying the thermal energy input FCAW work method in arc welding into the 3-pass model using the GTAW method.

Keywords: GTAW, FCAW, SS400 steel, Thermal elastoplasticity, Butt welding, Residual stress

Article History

Article Received: 24 July 2019

Revised: 12 September 2019

Accepted: 15 February 2020

Publication: 26 March 2020

1. Introduction

Welding is a core technology as well as a joining technique that is widely used in various industrial sites such as ships, automobiles and pressure vessels. In the shipbuilding industry, steel materials are mainly FCAW (Flux Cored Arc Welding), and non-ferrous materials and alloy steels are applied with gas tungsten arc welding (GTAW)[1,2]. These welding methods are classified as special welding, contributing to the

reduction of working time and quality uniformity. Recently, a welding method that can obtain high quality such as automated gas tungsten arc welding (GTAW) has been applied. The principle of gas tungsten arc welding (GTAW) welding is to weld the base metal by using arc heat between the non-consumable tungsten electrode and the base metal. GTAW is easy to apply to thin plate welding because it is easy to manage the heat input of welding. Tungsten electrode is non-

consumable, so it can be applied to most metal welding without any filler material. In addition, the mechanical properties and corrosion resistance of the weld is excellent, it is easy to weld non-ferrous metal, and the protective gas is transparent, the welder can understand the welding situation well. FCAW (Flux Cored Arc Welding) is a representative welding method of the consumable welding method in which the shielding material surrounds the core wire, the welding rod is supplied in an automatic or semi-automatic manner, and CO₂ gas is supplied from the outside to protect the welded portion. FCAW has less spatter, good appearance, and faster welding speed than GTAW or SMAW. However, FCAW is limited to the base metal of the iron system, and if the wind speed is more than 2m/s, windshield measures are required, and there is a disadvantage that a working environment should be created to sufficiently protect the protective gas[3,4,5].

1.1 Objectives

In this study, heat affected zone and heat distribution characteristics of specimens prepared with different welding methods and number of PASS layers were analyzed. In addition, we will examine the efficient method when joining SS400 mild steel by V-butt welding method.

2. Experimental Methods

• Thermal elasto-plasticity.

The welded structure has a locally high temperature difference due to the inflow of thermal energy, which causes plastic deformation and residual stress of the material. For this reason, welding analysis can be approached as a problem of temperature distribution analysis and thermal deformation analysis with increasing time, and it is assumed that heat transfer and elasto-plastic analysis proceed as the heat source progresses over time. The analysis of the temperature distribution of the welded structure due to the heat inflow of the moving heat source is expressed by

the heat diffusion equation, and the temperature distribution is calculated repeatedly over time increment[6,7]. In this study, a commercial finite element analysis program(MSC. Marc) was used. Heat transfer analyzes the progress of the heat source for each layer, and the ductile structural analysis was performed by substituting the thermal load for the thermal distribution and linking it with the elasto-plastic analysis. In this study, the heat flux was assumed to be the heat input energy distribution, and the thermal elasto-plastic analysis was carried out by dividing it into a 1-pass model using the FCAW method and a 3-pass model using the GTAW method. The heat source model is applied to Goldak's double ellipsoidal heat source, which is used for general arc welding analysis. The heat flux formula used the heat flux distribution function and the heat energy value. After the welding, there is a cooling step and it is necessary to prevent structure transformation due to heat, so the cooling conditions for this specimen were also set. The temperature of the specimen used in this study was 23 °C , and the conditions for cooling the surface of the specimen cooled at room temperature for a total of 1 hour were applied. In thermoelasto-plastic analysis, the properties of materials change greatly with temperature, and calculations require values above the melting point. Various physical properties according to the temperature change refer to the conventional research data.

• Sample preparation.

Specimens were fabricated using SS400 mild steel, which is widely used in industrial sites. The chemical composition and mechanical properties of the steel are shown in Table 1 and Table 2. The specimens were welded in two cases. In the first case, V-butt welding was performed on the test piece by applying manual GTAW. In the second case, the specimen was prepared by applying FCAW welding conditions to the same steel.

Table 1: Chemical composition of the SS400 mild steel

Elements Material	C	Si	Mn	P	S	Cr	Ni	Fe
SS400	0.15	0.19	0.42	0.012	0.021	-	-	Bal

Table 2: Mechanical properties of the SS400

Elements Material	Tensile strength (MPa)	Bending strength (MPa)	Hardness (MPa)
SS400	420	618	144

Table 3: Welding condition of the GTAW

Welding PASS (No.)	Output voltage(V)	Gas flow rate (liter/min.)	Welding Speed(sec.)
1	95	16	48
2	110	16	42
3	110	16	46

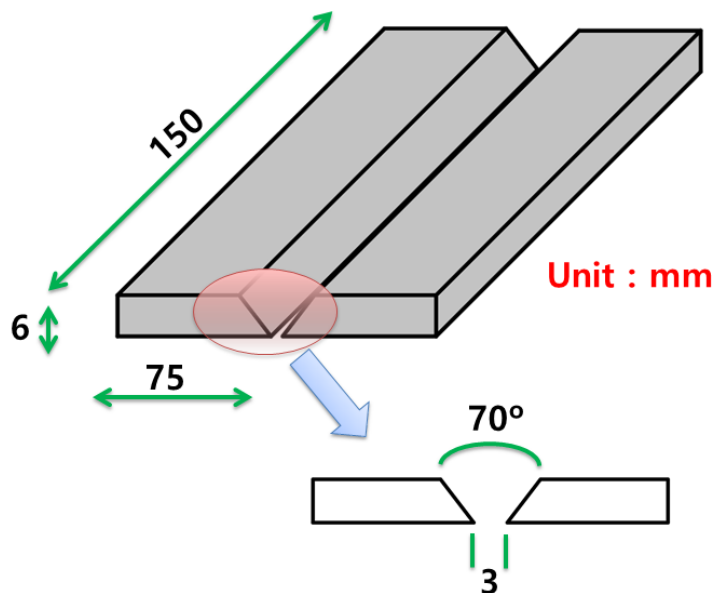


Figure 1. Schematic diagram of the base metal for GTAW.

Table 4: Welding condition of the FCAW

Welding PASS (No.)	Output voltage (V)	Output current (A)	Gas flow rate (liter/min.)	Welding Speed(sec.)
1	24	250	18	35

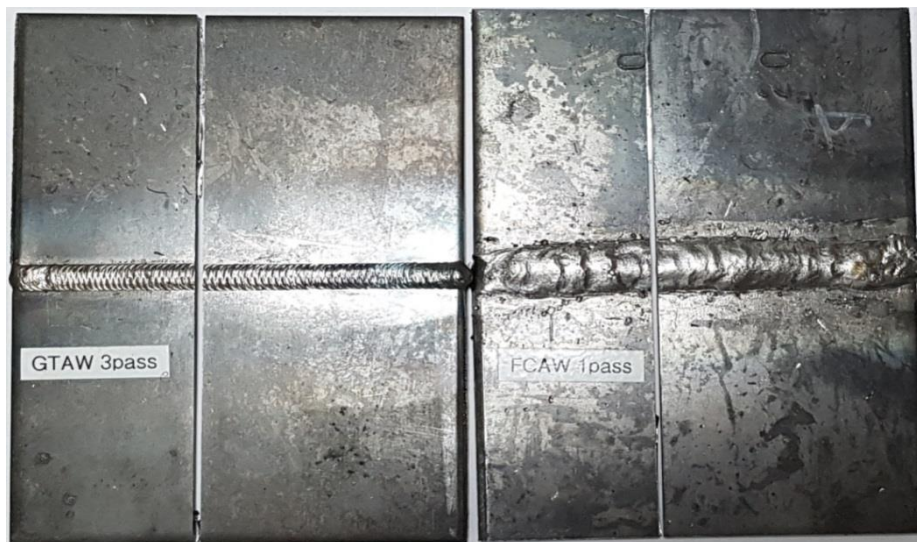


Figure 3. Two different specimens etched by corrosive solution (GTAW 3 PASS and FCAW 1 PASS).

The welded two specimens were cut and etched to the same cutting position for macro macroscopic inspection.

Welding was made by a welder over 20 years under the set conditions. Butt welding was performed with the same size specimen. The shape and detailed dimensions of the specimens are shown in Figure 1.

The welding conditions of the butt welded specimen by GTAW method are shown in Table 3. Specimens were welded after temporary welding using a TIG welding machine.

FCAW used CO₂ welder as shown Figure 2, welding conditions are the same as GTAW, and current and voltage are shown in Table 4. Normally, 2 passes were welded but 1 pass was welded for experiment.



Figure 2. FCAW welder for the butt welding(Worldwel Co.)

- **Thermal factors.**

The heat transfer and residual stress analysis of each specimen were carried out to observe the change of the structure due to heat. For the microstructure analysis, the specimens were cut 50 mm from the ends and again set a range of 30 mm from the center of the bead to collect 50 mm × 60 mm specimens. Generally, both ends of the welded part are excluded from cutting because the position where welding defect can occur. The center part is a part that connects the beads by replacing the welding electrodes in SMAW, and except this part, the 1/4 and 3/4 points of the specimen were cut and polished. The shape of the

cut specimen is shown in Figure 3. The cut surface of the welded specimen is ground in the order of sand paper identification number 160→200→400→600→800→1000→1200, and then polished using 1 μm-size alumina (Al₂O₃) abrasives. After polishing, corrosion was performed using 4% Nital etching solution. The cut specimens were etched with corrosive solution and visual observations were used to compare the differences between the macroscopic structures of the two samples. Mild steel is composed of pearlite and ferrite, but in this study, only weld beads and heat affected zones were observed macroscopically rather than metal microstructures.

3. Results

3.1. Thermal elasto-plasticity analysis

In the actual welding work, the specimen was free without restraint, but the condition of forcing restraint on the end of the specimen was selected to prevent the rigid motion that might occur during the analysis. The generation of weld beads

for weld analysis simulates the instantaneous element generation method where beads are generated when the heat source moves by applying activation and deactivation methods. GTAW set the next PASS to be generated at a time interval after 1-PASS considering the actual working environment[8,9].

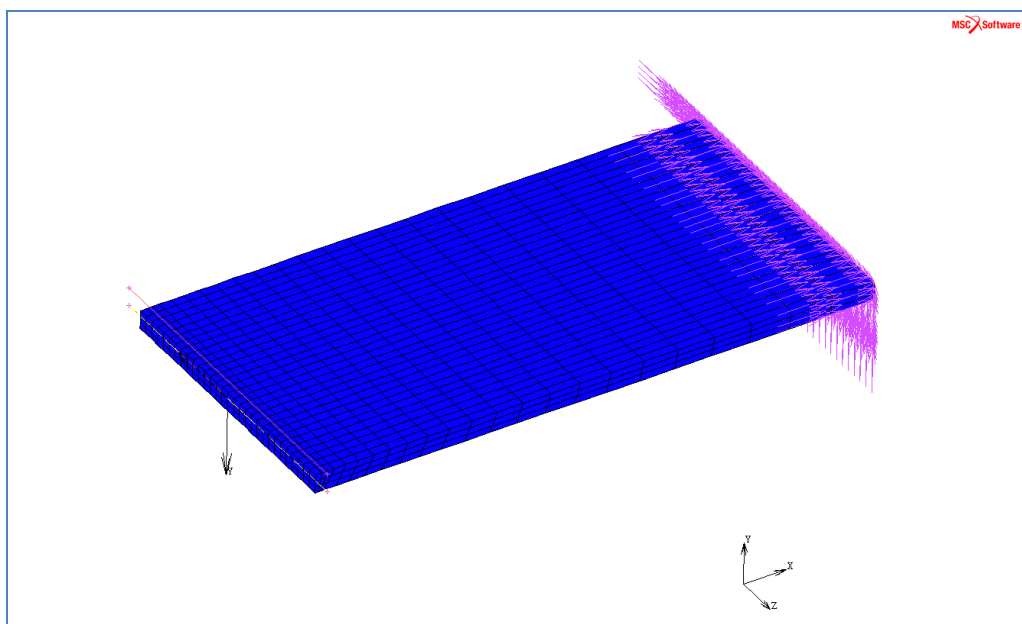


Figure 4. 1-PASS welding model.

On average, GTAW and FCAW showed temperature distribution of about 1600°C. After 1-PASS, the temperature dropped to about 900°C before the next PASS. In the next PASS, the

temperature increased about 3000°C, and when welding proceeded again, the temperature distribution was about 1600°C. The model used for the 1-PASS analysis is shown in Figure 4.

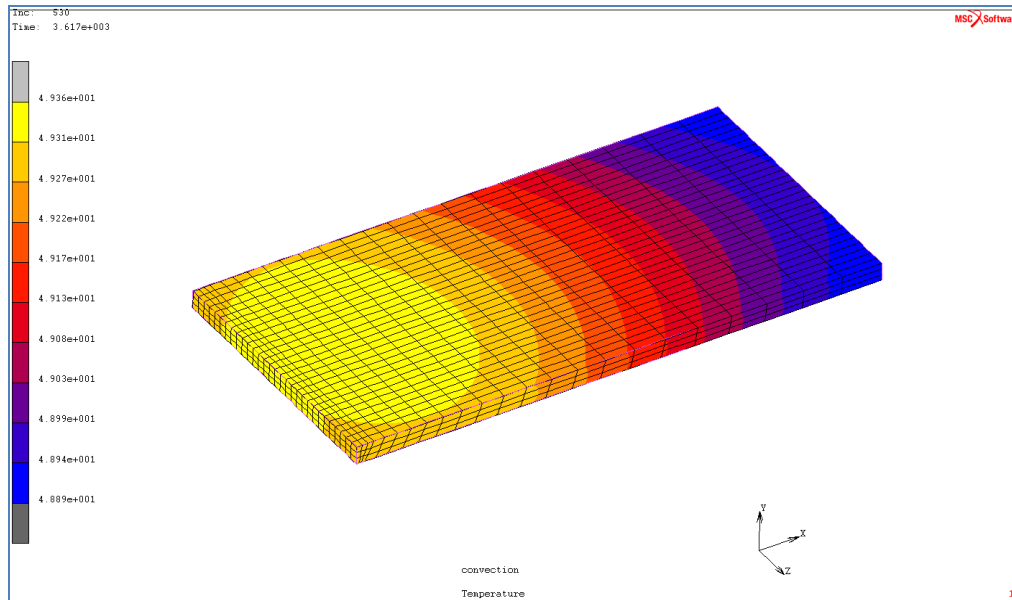


Figure 5. Expected temperature distribution of specimen after welding by applying 1-PASS model

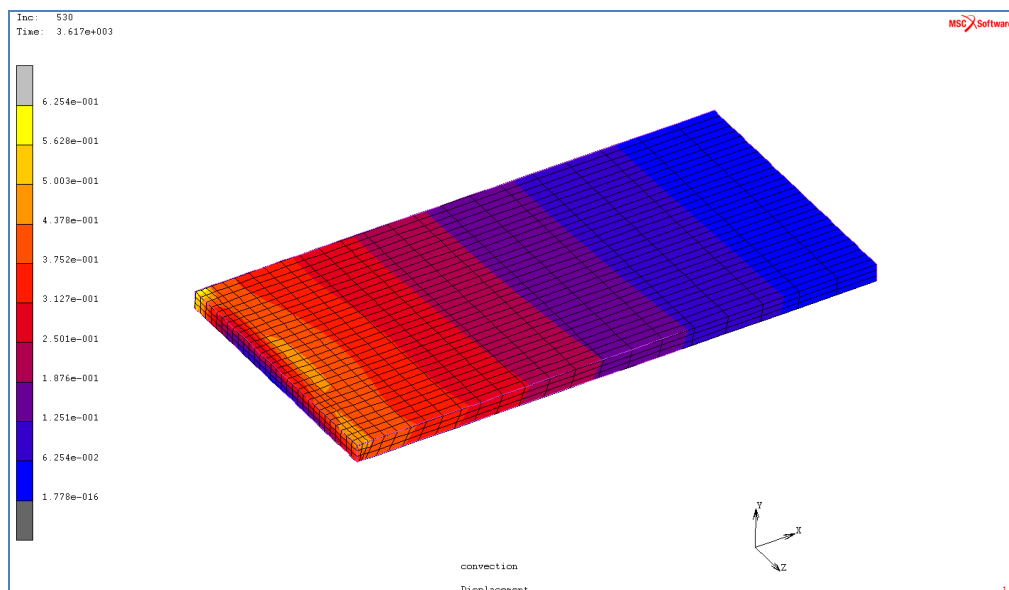


Figure 6. Expected deformation after weld using the 1-PASS model (unit: mm)

The welds were subdivided and the element size increased with distance from the weld[10]. As the constraint condition, the fixed condition was set at the end of the specimen, and the symmetry in the X direction was set based on the weld bead part. Figure 5 shows the temperature distribution of the

specimen after welding, as interpreted by the 1-PASS model[11]. Figure 6 shows the deformation values after welding by applying the 1-PASS model. Figure 7 shows the expected stress distribution of the specimen after welding using the 1-PASS model.

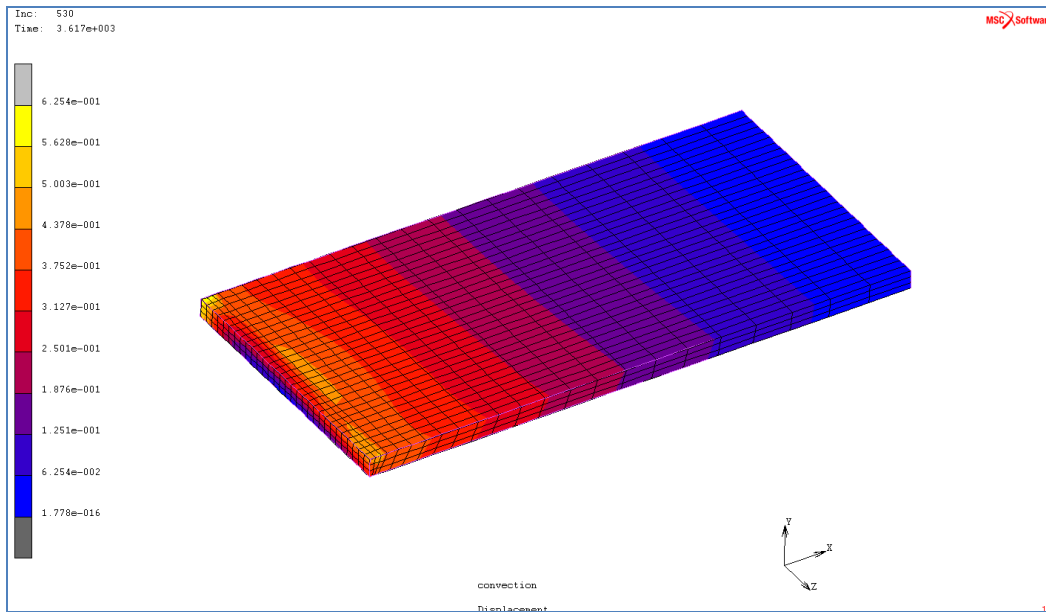


Figure 7. Expected stress distribution after weld using the 1-PASS model (Von-mises Stress, unit: MPa).

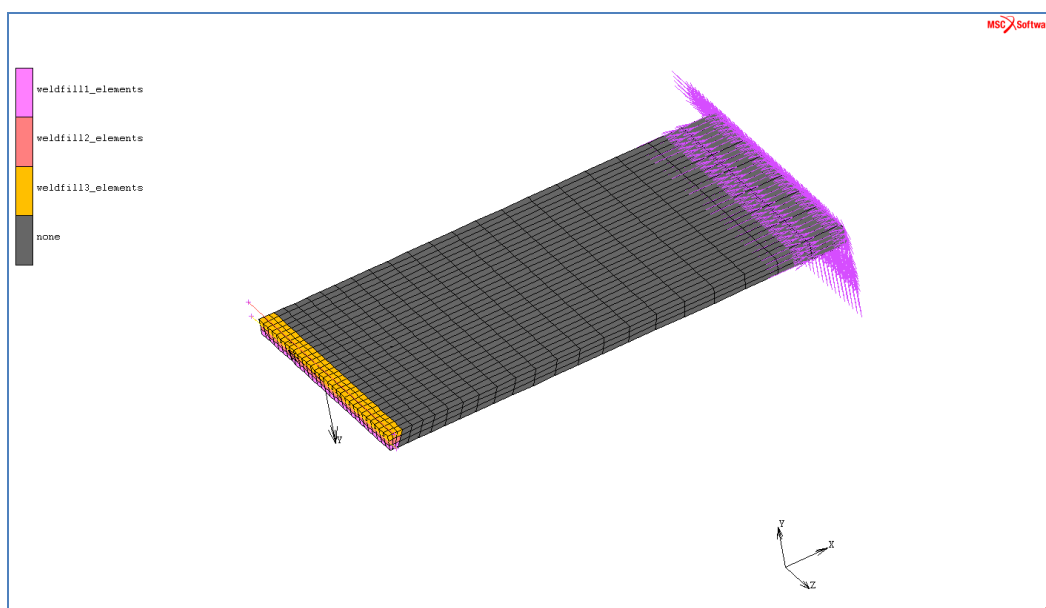


Figure 8. 3-PASS welding model.

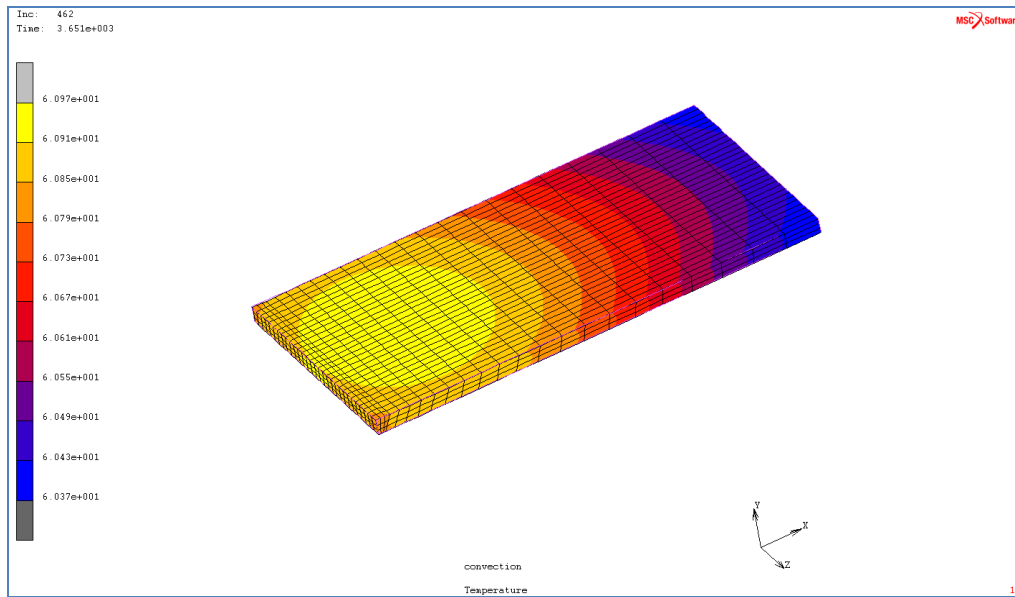


Figure 9. Expected temperature distribution of specimen after welding by applying 3-PASS model.

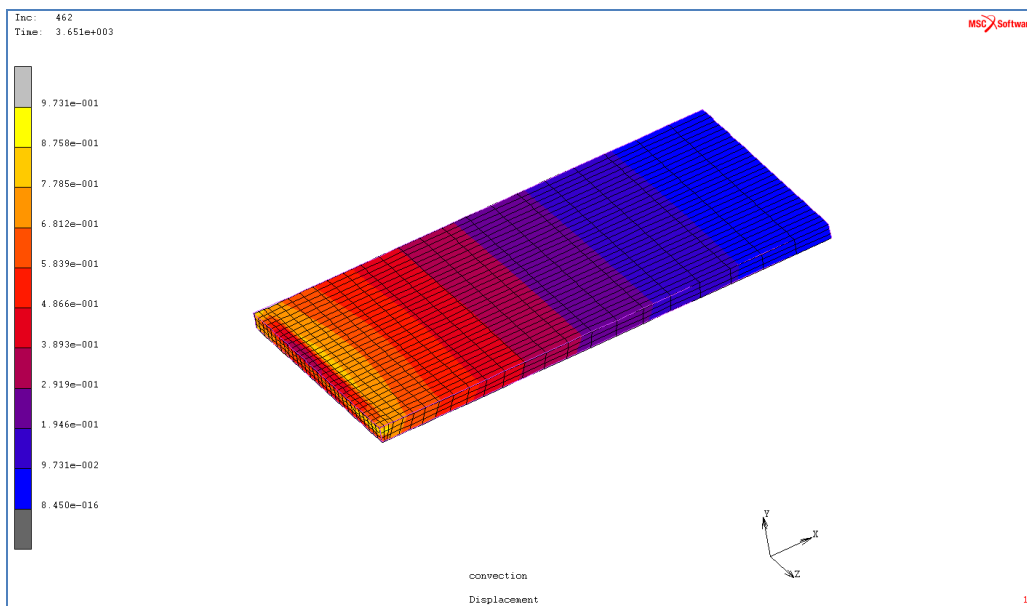


Figure 10. Expected deformation after weld using the 3-PASS model (unit: mm).

The model used for the 3-PASS analysis is shown in Figure 8. The model and constraints are the same as for the 1-PASS model. Figure 9 is shown Expected temperature distribution of specimen after welding by applying 3-PASS model.

The result of estimating specimen deformation after welding with 3-PASS model is shown in Figure 10.

Figure 11 shows the expected stress distribution of the specimen after welding using the 3-PASS model.

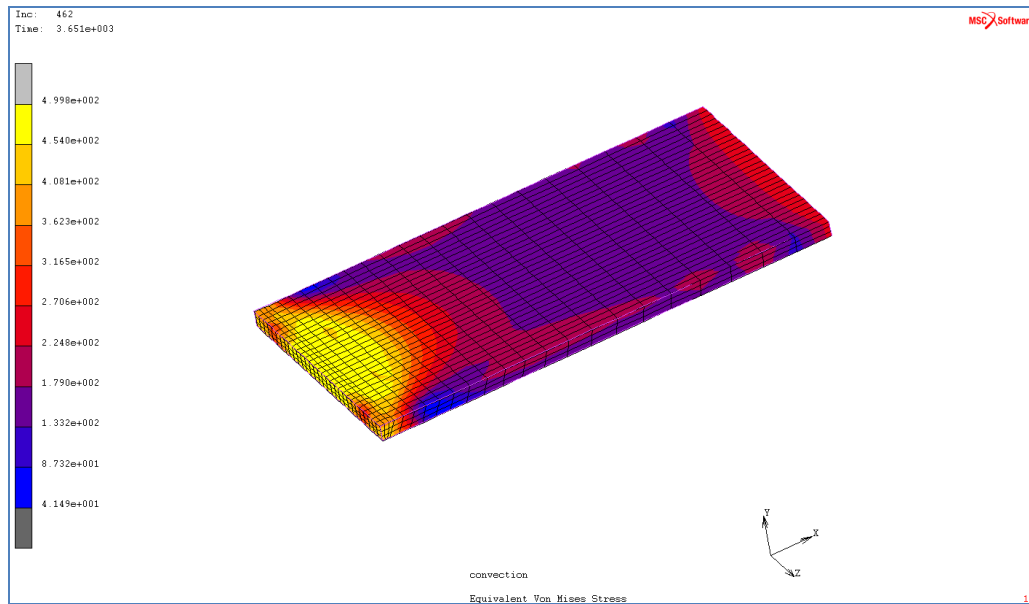


Figure 11. Expected stress distribution after weld using the 3-PASS model (Von-mises Stress, unit: MPa).

3.2. Thermal elasto-plasticity analysis

The results of analyzing the residual stress distribution of the weld specimen according to the

GTAW and FCAW welding methods are shown in Figure 12 and Table 6.

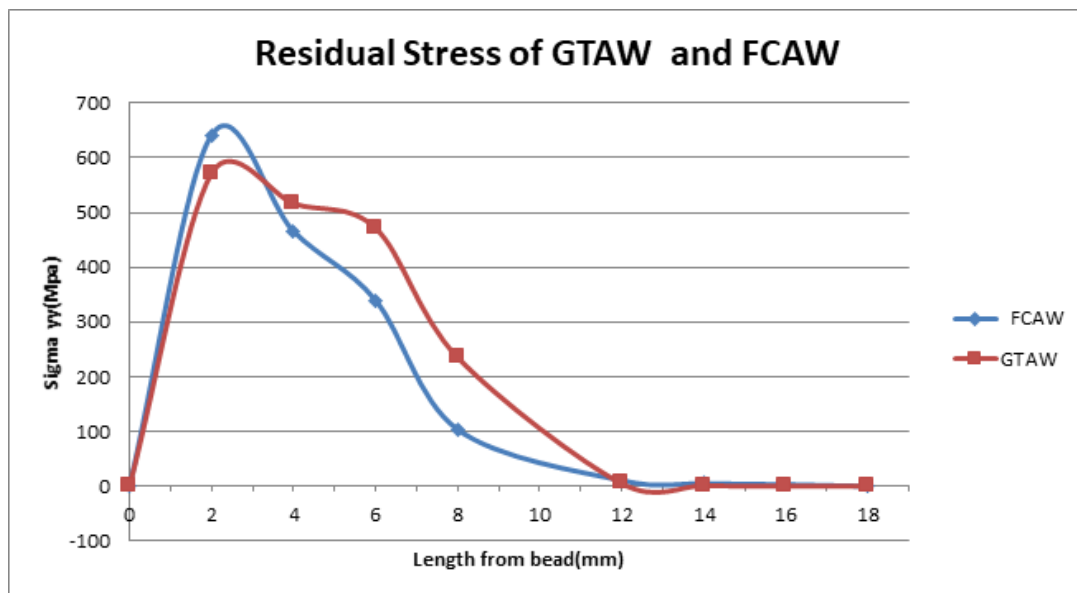


Figure 12. Residual stress distribution of the GTAW and FCAW process.

Table 6: Residual Stress with distance from bead by GTAW and FCAW process

Distance from bead (mm)	FCAW	GTAW
	Sigma yy(Mpa)	
0	0	0
2	640.83	570.12
4	465.3	515.2
6	339.57	470.56
8	103.84	234.9
12	10.61	5.00
14	5.10	1.10
16	3.30	0
18	0	0

The element length of the welded specimen model is about 1 mm in size and represents the stress values measured for each of the two elements (2 mm). Although the FCAW method was welded in one pass, the higher residual stress resulted in the higher current value among the welding conditions[12,13].

The residual stresses of the specimens using the two welding methods did not show any significant

difference, but the residual stresses were higher in the FCAW method than in the GTAW method. In general, high tensile stress is concentrated around the weld bead, but as the distance from the bead increases, the tensile stress decreases.

The results of this field study showed that the finite element analysis result of comparing the tensile strength of welding material was slightly higher[14].



Figure 13. Sectional appearance of the etched specimens by GTAW and FCAW process.

4. Conclusion

In this study, we investigated the thermal factors according to the welding method and the number of PASS when welded SS400 steel by butt welding. In the structure test results, we compared the heat affected zone and heat distribution characteristics of each specimen. We also compared the advantages and disadvantages of each welding method in terms of efficiency using heat transfer and residual stress results from 3D finite element analysis. FCAW specimens show higher residual stresses than GTAW specimens due to the high current applied to the weld. Increasing the number of welding pass did not show any significant residual stress, and the number of welding pass was not proportional to the residual stress. If welding with a large current, the time required is reduced, but the residual stress can be increased. Therefore, a proper work considering the base metal and the welding shape is required. In the future, we will study the effect on the safety of structures such as ships based on the results of this study.

5. Acknowledgment

This study was supported by research funds from Nambu University.

References

- [1] Singh B, Singhal P, Saxena KK. Investigation of Thermal Efficiency and Depth of Penetration during GTAW Process. *Materials Today: Proceedings*. 2019 Jan 1;18:2962-9.
- [2] Oktadinata H, Putra AG. microstructure and hardness profile of dissimilar lap joint of type 304 stainless steel to SS400 carbon steel. *Metal Indonesia*. 2019 Dec 31;41(2):47-54.
- [3] Cho BJ, Lee SJ. Evaluation of Mechanical Test Characteristics according to Welding Position in FCAW Heterojunction. *Journal of the Korea Academia-Industrial cooperation Society*. 2019;20(8):649-56.
- [4] Karakizis PN, Pantelis DI, Dragatogiannis DA, Bougiouri VD, Charitidis CA. Study of friction stir butt welding between thin plates of AA5754 and mild steel for automotive applications. *The International Journal of Advanced Manufacturing Technology*. 2019 Jun 19;102(9-12):3065-76.
- [5] da Silva MS, Souza D, de Lima EH, Bianchi KE, Vilarinho LO. Analysis of fatigue-related aspects of FCAW and GMAW butt-welded joints in a structural steel. *Journal of the Brazilian Society of Mechanical Sciences and Engineering*. 2020 Jan;42(1):1-3.
- [6] Tervo H, Kajalainen A, Pallaspuro S, Anttila S, Mehtonen S, Porter D, Kömi J. Low-temperature toughness properties of 500 MPa offshore steels and their simulated coarse-grained heat-affected zones. *Materials Science and Engineering: A*. 2020 Jan 31;773:138719.
- [7] Gunawan E, Choifin M, Rosidin MK, Afifah YN, Lestariningsih W, Pradana MS, Prasnowo MA, Makki A. Analysis of the Effect of Current Flow Variations in GTAW on SS 400 Plate Material Connected with SUS 304 Stainless Steel Plate Against Tensile Strength and Hardness with ER308L Electrodes. *InJournal of Physics: Conference Series* 2019 Mar (Vol. 1175, No. 1, p. 012277). IOP Publishing.
- [8] Purnama D, Oktadinata H. Effect of Shielding Gas and Filler Metal to Microstructure of Dissimilar Welded Joint Between Austenitic Stainless Steel and Low Carbon Steel. In *IOP Conference Series: Materials Science and Engineering* 2019 Aug (Vol. 547, No. 1, p. 012003). IOP Publishing.
- [9] Purnama D, Oktadinata H. Effect of Shielding Gas and Filler Metal to Microstructure of Dissimilar Welded Joint Between Austenitic Stainless Steel and Low Carbon Steel. In *IOP Conference Series: Materials Science and Engineering* 2019 Aug (Vol. 547, No. 1, p. 012003). IOP Publishing.
- [10] Park JH, Kim SH, Moon HS, Kim MH. Influence of Gravity on Molten Pool Behavior and Analysis of Microstructure on Various Welding Positions in Pulsed Gas Metal Arc Welding. *Applied Sciences*. 2019 Jan;9(21):4626.

- [11] Kikani P. Analysis of Process Parameters for Dissimilar Metal Welding Using MIG Welding: A Review. *Journal of Material & Metallurgical Engineering*. 2019 Apr 10;6(2):38-41.
- [12] Kimapong K, Triwanapong S. Effect of GMAW Shielding Gas on Tensile Strength of Dissimilar SS400 Carbon Steel and SUS304 Stainless Steel Butt Joint. In *Materials Science Forum 2019* (Vol. 950, pp. 70-74). Trans Tech Publications.
- [13] Rakesh N, Rameshkumar K, Mohanan A, Valsan KV, Sandeep S, Prasad H. Numerical modeling of Flux assisted Gas Tungsten Arc Welding (F-GTAW) process of Duplex Stainless Steel (DSS). In *Journal of Physics: Conference Series 2019 Mar* (Vol. 1172, No. 1, p. 012019). IOP Publishing.
- [14] Peshkov I, Boscheri W, Loubère R, Romenski E, Dumbser M. Theoretical and numerical comparison of hyperelastic and hypoelastic formulations for Eulerian non-linear elastoplasticity. *Journal of Computational Physics*. 2019 Jun 15;387:481-521.
- [15] Lee JH, Jang BS, Kim HJ, Shim SH, Im SW. The effect of weld residual stress on fracture toughness at the intersection of two welding lines of offshore tubular structure. *Marine Structures*. 2020 May 1;71:102708.